Characteristics of Platinum on Zeolite Electrocatalyst for Direct Methanol Fuel Cell

Jun Yao[1*] and Yufeng Yao[2]

[1]School of Engineering, University of Lincoln, Brayford Pool, Lincoln, LN6 7TS, UK
[2] Faculty of Science, Engineering and Computing, Kingston University, Friars Avenue, London SW15 3DW, UK

Characteristics of Platinum (Pt) on zeolite electrocatalysts have been experimentally studied to understand its potentials for direct methanol fuel cell (DMFC) applications. The Y zeolite was chosen as a Pt-supported substrate with 1.5 wt% Pt loading on zeolite. The Pt nanoparticle size and local atomic structure in both electrochemical and gas cell treatments were investigated by using X-ray absorption spectroscopy (XAS), in particular the extended X-ray adsorption fine structure (EXAFS) method, and the electrocatalytic activity of Pt nanoparticle on Y zeolite was determined by cyclic voltammetry (CV). Studies were focused primarily on the observation of hydrogen adsorption and desorption in the hydride region, where the presence of H^+ ions was critical for such a process occurred. Analyses have shown that the Pt oxides can be electrochemically reduced, due to a hydrogen 'spillover' phenomenon throughout zeolite structures. Based on theoretical estimation and EXAFS data fitting, it was found that the Pt nanoparticle size was 1-1.1 nm from gas cell treatment and 0.7 nm from electrochemical cell treatment. For both scenarios, the number of atoms was estimated 147 and 55 respectively, with 13 atoms at the edge of a Pt cluster for an icosahedron structure. This study demonstrated that the Pt catalytic site on zeolite can be electronically accessible; despite that zeolite is a dc insulator. The Pt/Y zeolite as a new type of electrocatalyst has shown some promises for industrial-scale fuel cell applications, such as reducing higher electrode cost and/or overcoming the difficulty of electrolyte separation.

Keywords: Pt on Y zeolite catalyst, Nanoparticle, EXAFS, Fuel Cell.

Received 01 June 2011; Accepted 31 August 2011

1. INTRODUCTION

Zeolite-supported noble metals (e.g. Platinum) as catalyst are widely used in many commercially important applications, because of its catalytic activity and higher selectivity. More recently, there is growing interest to apply this type of catalyst for fuel cell applications, ranging from fuel conversion and conditioning to membrane additives [1]. For direct methanol fuel cell (DMFC) applications in particular, the Platinum carbon (Pt/C) has been used as an electrocatalyst to reduce the usage of noble metal Pt. The normal Pt loading on a Pt/C electrocatalyst is about 20% ~ 40%, which is not only prohibitively expensive, but also can possibly lead to larger metal particle sizes that will decrease the electrocatalytic activity. Thus, it is necessary to develop feasible techniques that can produce highly dispersed Pt nanoparticles on a chosen substrate, in order to reduce the Pt usage. A previous study of Min et al. [2] has demonstrated the possibility of reducing Pt quantity by increasing surface area of Pt nanoparticle on a substrate.

Zeolite is a suitable material to host Pt, because it is capable of acting as a solution like ionic conduction [3]. Zeolite tetrahedral SO_4 and AlO_4 structure units can create the interconnecting channels that offer a great capacity for metal ions exchange to give the desired cationic form [1] and lock Pt nanoparticles into the desirable positions at a certain temperature range [4] without damaging its crystalline lattice during calcinations. While the advantages of using zeolite to produce the nano-sized metal particle to reduce the cost are

* Corresponding author, email: jyao@lincoln.ac.uk

impressive, the disadvantages of lacking a dc electronic conduction will cause some difficulties in exploring underlying mechanisms of how the electrochemical oxidation and reduction occur for metal particles being trapped in the zeolite structure, such as the particle aggregation that prevents electrolyte inserted into the pores' structure to contact Pt catalytic site for ionization [5].

The electrocatalytic ability of Pt/Y zeolite catalyst can be explained by hydrogen (H^+) ions 'spillover' phenomenon associated with Pt catalytic sites in the zeolite structure. A 'spillover' occurs when the electrochemical reaction takes place during the surface diffusion process of the absorbed species [6] and migrates into the Pt catalytic sites on zeolite framework. Previous study by Wen et al. [7] on a Pt/C electrocatalyst revealed that the 'spillover' of hydrogen atoms on Pt/C electrode happened during surface diffusion and hydrogen (H^+) ions were able to form the acidic surface oxides of carbon where the carbon black was a main substrate on the electrode surface. Hydrogen 'spillover' has also been found in gas phase. For example, the research work done by Fujimoto [8] showed that hydrogen 'spillover' could occur from Pt catalytic sites to the zeolite acidic site, the so-called Bronsted and Lewis acidic sites. However, hydrogen 'spillover' on the Pt/Y zeolite electrode in the electrochemical environment has not been fully investigated yet. Boyanov et al. [9] studied Pt/Y zeolite interaction by an EXAFS experiment and found that the disorder level of Pt on zeolite framework had a dramatic effect on the electronic structure of Pt. Yokoyama et al. [10] also revealed that the Pt-Pt bond distance of a Pt cluster encaged in the zeolite supercages was shorter than that in the bulk Pt metal. These investigations suggested that the charger transfer from Pt clusters to the substrate was stronger in the Pt/Y zeolite electrocatalyst than other Pt catalysts. The contraction of Pt-Pt bond distance on zeolite was due to the increase of Pt-Pt bonding energy caused by electron deficiency. Previous study of Koningsberger et al. [11], using EXAFS data, has predicted the Pt metal particle size with the first shell Pt - Pt coordination numbers of 5.5, and the metal particle having approximately 15 atoms on average in fitted shells. The predicted Pt-Pt distance was 2.75 Å, indicating the characteristics of metallic nature of the bulk Pt. They have concluded that oxygen atom inherited from the zeolite framework did have significant influences on the charger transfer.

The aim of this paper is to study how electron transfer reactions can occur at nano-scaled metal particles such as Pt on a substrate (e.g. Y zeolite) under electrochemical control using cyclic voltammetry (CV) measurement and X-ray absorption spectroscopic (XAS) techniques, in particular the extended X-ray absorption fine structure (EXAFS) method. The electrocatalytic activities of Pt - Pt bond particles will be investigated as a function of Pt particle size and its neighbouring distance using EXAFS experiment. The cyclic voltammetry measurement will be performed to ascertain the influence of hydrogen adsorption and desorption processes on Pt catalytic sites for hydrogen oxidization and reduction. Hence, the electro-activities of the catalyst of interest on the electrodes can be accurately determined.

2. EXPERIMENTAL PROCEDURE

2.1. Preparation of Pt/Y zeolite electrocatalyst

An appropriate quantity of $Pt(NH_3)_4(NO_3)_2$ salt was dissolved in 200 ml of triply distilled water at 0.004 mol dm^{-3}, and agitated in an ultrasonic bath for 20 minutes. The sodium Y zeolite powder was dispersed in 1 dm^3 of triply distilled water using a water-jacketed reactor. Meanwhile, the Pt salt solution was added slowly at a flow rate of 0.1 ml/min into the reactor containing NaY zeolite slurry with zeolite concentration of 1 gram per 100 ml. The temperature of the ion exchange solution was maintained at 70 ^oC for a few hours. The sample was later filtered and washed with copious amount of triply distilled water until no $[Pt(NH_3)_4]^{2+}$ complex being detected by UV spectrum at 290 nm, similar to a previous study [12]. The washed sample was then placed in an oven for drying at 100 ^oC to 120 ^oC.

2.2. Calcination and Reduction

The syntheses of Pt microstructures on Y zeolite followed a method developed by Gallezot and co-workers [13]. The calcination and reduction processes were performed in a fluidized bed reactor. For calcination, a mass of 2g ion exchanged Pt/Y zeolite was placed on the reactor bed with 10 μm pore glass frit. The argon was introduced at a flow rate of 250 ml/min into the reactor from the bottom to provide the maximum contact surface area between the Pt/Y zeolite catalyst and Ar gas. Meanwhile, the furnace was heated up to 150 ^oC at a heating rate of 1 ^oC/min and the Pt/Y zeolite was maintained in argon for overnight. While sample was cooled down, oxygen (O_2) was introduced into the reactor at a flow rate of 200 ml/min. Sample was then re-heated up to 350 ^oC at a heating rate of 0.3 ^oC per min. For reduction, the reactor heating rate was controlled at a constant 5 ^oC/min and sample was gently purged with a gas mixture of $5\%H_2/95\%N_2$ at a flow rate of 1L/min for 12 hours. The reduction temperature was maintained at 400 ^oC to produce finer Pt nanoparticles distributed on zeolite. Bergeret et al. [14] discovered that at certain temperature, the reduction process could cause the agglomeration of Pt atoms in the supercages, and the Pt nanoparticles could even migrate and extend over several cages at a higher temperature. The elimination of isolated Pt atoms entrapped in the sodalite cages by forcing them migrated back into the supercages is a very challenge task. The location of Pt nanoparticles is mainly dependent on the calcination process [15].

2.3. Nafion@ Bound Electrodes

The electrode with porous structure can provide some significant advantages for mass transport that is crucial for electrochemical reaction to take place. In order to achieve uniformly dispersed catalyst and eliminate any possible resistance on the electrode, the Nafion@ based conductive electrolytic polymer has been employed as a binder for an in-house electrode preparation. The Pt/Y zeolite catalyst and XC-72R carbon mixture were grounded to a fully mixed powder. The appropriate amount of 15wt% Nafion@ was dropped in to a small volume of water and then the solution was added to the prepared powder mixture. The resultant paste was agitated in an ultrasonic bath until well mixed before spreading onto a typically 9 cm^2 carbon paper sheet (e.g. E-TEK TGHP-90). The sheet was pressed at a temperature of 100 ^oC and a pressure of 75 kg cm^{-2} for 3 minutes. The electrode was cut to a disc size of 1.3 cm^2 for cyclic voltammetry (CV) measurement and 2.5 cm^2 for in-situ EXAFS experiment.

2.4. Cyclic Voltammetry

The charge separation on Pt was investigated in an electrochemical cell consisted of a Pt/Y zeolite working electrode, a counter electrode and a reference electrode, in which the counter electrode was a platinum gauze with a large surface area to provide the reverse reaction response to working electrode, and also to ensure that polarization effect can be neglected. The Hg/Hg_2SO_4 (MMS) reference electrode was placed in a Luggin capillary. The tip of Luggin capillary was positioned as close as possible to the working

electrode to avoid the large iR losses between the working and the counter electrodes. The electrolyte solution was 2.5 mol dm^{-3} sulphuric acid and the overall electrolyte volume was measured at 150 cm^3. The electrolyte solution was purged with nitrogen and was thoroughly stirred to remove all dissolved oxygen in the test cell before cyclic voltammetry (CV) measurement. The CV measurement was conducted using a computer-based Autolab PGSTAT20. The working electrode was controlled by a potentiostat that changed continuously at a constant scan rate (dE/dt) of 1 mV/s by a potential ramp from a waveform generator [16]. The oxidation and reduction of the electro-active species on the Pt/Y zeolite electrode was detected by a current change in a potential region of -0.65 V ~ +0.5 V, where no solvent and electrolyte decompositions were occurred [17].

2.5. EXAFS Experiment

The Extended X-ray Absorption Fine Structure (EXAFS) experiment was performed by employing the Synchrotron Radiation Source (SRS) at Daresbury Laboratory, UK. The wiggler beam line was operated at 2 GeV with an average current of 220 mA. The harmonic higher-order signals that affected the amplitude of EXAFS were removed using a double crystal Si220 monochromator. The 50% detuning of harmonic beam was used to locate the Pt L_{III} absorption edge. The intensities of incident and transmitted beams were measured using a gas-filled ion chamber with Ar, Xe or Kr and He gases. The reference sample was a Pt foil with the first shell Pt–Pt distance 2.76 Å. The electrochemical cell used for in-situ EXAFS experiment was formed by two acrylic discs with the centre of discs being cut to create two Kapton windows for X-rays passing through to the electrodes. The working electrode was placed at the centre of one acrylic disc, and a gold-wired current collector was placed underneath the Pt/Y zeolite working electrode to reinforce the contact in the cell. The Pt gauze was employed to act as a counter electrode. Several layers of filter paper pre-soaked in 1 mol dm^{-3} H_2SO_4 solution were placed over the Pt/Y zeolite working electrode to prevent electrode drying out during the cell assembly. The MMS reference electrode was connected to the cell via a salt bridge. The electrochemical cell was re-assembled for EXAFS experiment to produce a sufficiently large absorption edge of $\mu\chi > 0.3$, where μ is the mass absorption coefficient and χ is the thickness of sample.

3. RESULTS AND DISCUSSION

3.1. Ex-situ EXAFS for 1.5 wt% Pt/zeolite electrocatalyst

The pellet employed for ex-situ EXAFS experiment was made using Pt/Y zeolite catalyst and boron nitride powder mixture. It was placed between two pieces of plastic film in a gas treatment cell. The EXAFS data was collected in air and hydrogen gases at a room temperature, respectively. The EXAFS spectrum was taken at the Pt L_{lll} edge and data analysis was carried out using software EXCURV 98 provided by Daresbury Laboratory.

Figure 1 depicts the EXAFS spectrum data and their Fourier transforms, fitted at R-space and k^3 weighting. From the Chi data $k^3\chi(k)$ plot, it is clear that the tendency of oscillation amplitude of raw EXAFS data is similar for 1.5 wt% Pt/Y zeolite catalyst sample being treated in air (i.e. 15ancr4/air) or in hydrogen (i.e. 15ancr4/H_2). This suggests that on average each Pt nanoparticle has a longer neighbouring distance and higher Z (i.e. atomic number) neighbours due to a short oscillation period. For 15ancr4/air sample, the maximum peak of Fourier transform (FT) in R-space was 2.7 Å with neighbouring higher shell dominated by peaks between 4 Å and 6 Å. The dashed lines are the fitting results of the raw data. One Pt-O shell (i.e. the first shell) was observed with approximately coordination number of 1.23 and the Pt-O distance of 2.02 Å. The Pt-Pt distance in the Pt first shell was 2.76 Å. The fitting results for Pt coordination number were extended up to the Pt fourth shell.

For 15ancr/H_2 sample, hydrogen reduction (see Fig. 1b) has shown a significant effect on local Pt nanoparticle structure. There was no oxygen atom in the first shell and the Pt–Pt distance was 2.75 Å in the first shell, indicating the metallic nature of Pt nanoparticles with f.c.c structure of the bulk Pt. The Pt-Pt coordination number (N) in the first shell was 6.33, a factor of 2 higher than that found in 15ancr4/air (i.e. shell 2 in Table 1a). In both cases, the Pt-Pt was fitted up to 4 shells. The overall Pt-Pt coordination numbers in hydrogen was 17 atoms, higher than that in air (i.e. 14.83 atoms).

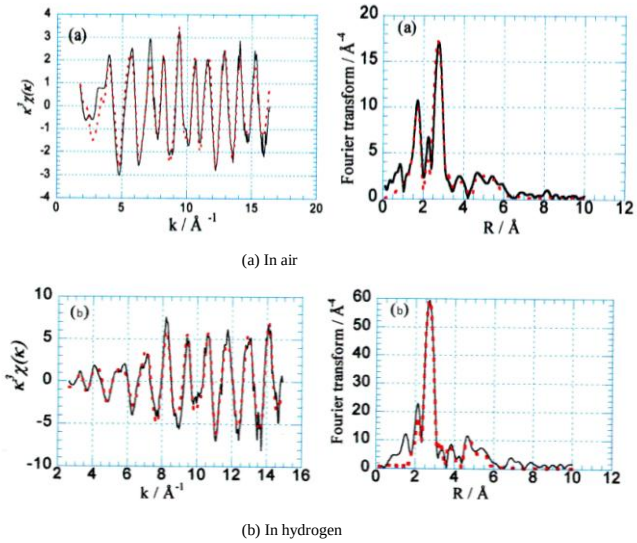

(a) In air

(b) In hydrogen

Fig. 1. EXAFS data fitting for 1.5 wt% Pt/Y zeolite catalysts (a) in air; (b) in hydrogen with phase corrected with experimental data in black solid line and the fitted data in red dashed line.

Table 1 presents the data fitting results for each Pt shell of catalyst chemically oxidation and reduction in air (15ancr4/air) and in hydrogen (15ancr4/H_2), respectively. N is average coordination number, and R is distance between neighboring shells.

Table 1. Data fitting results for each Pt shell.

(a) In air

15ancr4/air	Shell 1 O	Shell 2 Pt	Shell 3 Pt	Shell 4 Pt	Shell 5 Pt
N	1.23	3.13	1.75	3.12	6.83
R (Å)	2.02	2.76	3.90	4.81	5.44

(b) In hydrogen

15ancr4/H_2	Shell 1 Pt	Shell 2 Pt	Shell 3 Pt	Shell 4 Pt
N	6.33	0.88	3.34	6.40
R (Å)	2.75	3.91	4.78	5.42

3.2. BET Measurement and XRD Characterization

As EXAFS analysis was unable to identify zeolite crystalline structure, BET surface area measurement and XRD characterization were employed to understand the blocking pores on zeolite and also the change of the zeolite crystalline structure. Figure 2 gives BET surface area measurements. Comparing to a plain zeolite without Pt,

a 1.5 wt% Pt/Y zeolite has smaller surface area, indicating that due to precursor thermal treatment, the deposition of Pt on zeolite will cause the blocking pores phenomenon occurred. Hence, zeolite surface area can be decreased significantly by max 540 ~ 590 cm^2 g^{-1}. During the hydrogen reduction process the Pt nanoparticles can even be mobilized and migrated to block other zeolite opening pores.

The X-ray diffraction (XRD) spectra have been used to examine the zeolite crystalline structure differences between a plain zeolite and a 15ancr4 electrocatalyst zeolite. The data were collected as a function of angle of 2θ in a range of 5 ~ 44 degrees at a room temperature, where θ is the angle of incident or reflected X-ray beam. Comparing to that of a plain zeolite [16], the XRD pattern of a 15ancr4 electrocatalyst has shown significantly reduced diffraction peak intensity by maximum a factor of 10, but with slightly shifted peak positions. While the peak intensity decrease indicates the loss of zeolite crystallite, the XRD spectra exhibits similar patterns for two types of zeolites, confirming that the structural change due to the Pt metal loading is not very significant.

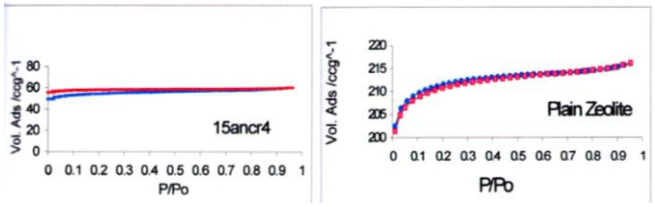

(a) 15ancr4 (b) plain zeolite

Fig. 2. Volumetric uptake of nitrogen at 77 K with absorption in blue dotted line, and desorption in red dotted line.

3.3. Cyclic Voltammetry Measurement

The cyclic voltammetry (CV) measurement was performed in an electrochemical cell to determine the electro-activity of species in solution and on electrode surface. It monitored the response of an electrochemical reaction by measuring current and potential changes. To understand and quantify the electrocatalytic activity of 1.5 wt% Pt loading on zeolite (15ancr4), a 5 wt% Pt loading electrode made from a commercial available 40 wt% Pt/XC-72R carbon catalyst mixed with extra XC-72R carbon, as seen in figure 3, was used for comparison investigations.

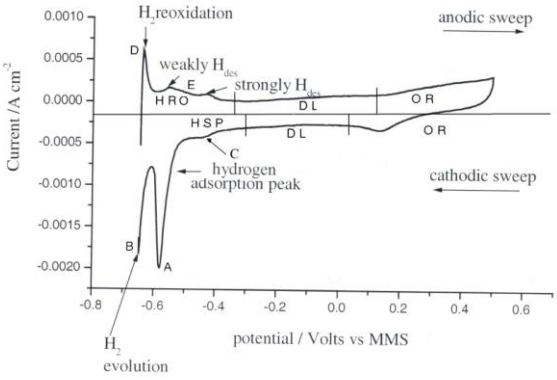

Fig. 3. Steady state CV of 5 wt% Pt/XC-72R electrode prepared by 40 wt% Pt/XC-72R with extra plain XC-72R carbon at a scan rate of 1 mV/s in 2.5 mol dm^{-3} H_2SO_4.

In general, CV can be distinguished in three regions: (1) hydride region of the cathodic sweep (-0.32 V ~ 0.65 V) and anodic sweep (-0.65 V to -0.36 V); (2) oxide region of the anodic sweep (0.12 V to 0.5 V) and cathodic sweep (0.5 V to 0.02 V); (3) the double layer of the anodic sweep (-0.36 V to 0.12 V) and cathodic sweep (0.02 V to -0.32 V), respectively. The hydride region starts at the point of hydrogen adsorption potential (HSP), sweeps in negative direction to -0.65 V, and cycles back to the hydrogen re-oxidation (HRO) region. Two significant features, hydrogen adsorption and desorption are determined with peaks assigned to hydrogen atoms at two different Pt surface sites. Peak A is believed to be caused by strong adsorption of H^+ ions due to their high adsorption energy on Pt catalytic sites. Peak C is attributed to weak adsorption of hydrogen. It is thought that H^+ ions have formed covalent bonding on Pt catalytic sites. Peak B is due to hydrogen evolution. Peak D is thought to be hydrogen re-oxidation, and peak E represents hydrogen ions desorption process. A current increase occurs in an oxidation region (OR) at a potential of 0.12 V to 0.5 V, due to the formation of Pt oxide species at the electrode surface. The oxide-stripping occurs in cathodic sweep in a potential region of 0.5 V to 0.02 V. For a potential from 0.02 V to -0.36 V and -0.36 V to 0.12 V, there are the double layer regions, attributed by charger separation between the plane of Pt metal surface and the electrolyte solution.

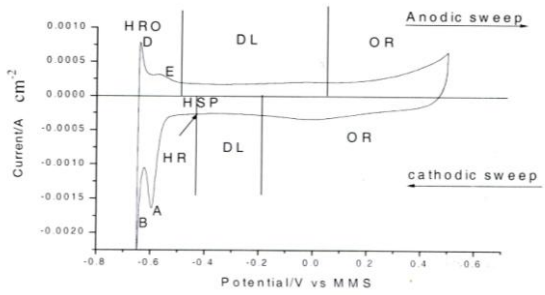

Fig. 4. A typical CV of 1.5 wt% Pt/Y zeolite (15ancr4) obtained at a scan rate of 1 mV/s in 2.5 mol dm^{-3} H_2SO_4.

Figure 4 displays a typical CV measurement of a 1.5 wt% Pt/Y zeolite working electrode, on which electrochemical oxidation and reduction processes were taken place. The potential sweep region was confined between -0.65 V and 0.65 V using a sweep rate of 1 mV/s. The evidence of electrochemical activity on Pt nanoparticles was detected in the hydride region between -0.45 V and -0.65 V. Although only one hydrogen adsorption peak, representing a strongly bounded Pt catalytic site, has been observed at -0.6 V, this does not mean that there was no weakly bounded Pt catalytic site exists. It is possible that both weakly and strongly bounded hydrogen may adsorb similar amount of energy, so that it was difficult to distinguish them unless a much slower sweeping rate, e.g. less than 1 mV/s, being used. Further decreasing a potential to -0.65 V, hydrogen evolution occurred. In the anodic sweep, one peak was measured at -0.64 V due to re-oxidation of hydrogen. The second peak was also found at -0.56 V due to hydrogen desorption. An oxidation current was recorded in a potential region of 0 V to 0.5 V in the cathodic sweep with a small peak determined at 0 V, due to removal of Pt oxides. Compared to the measurement of 5 wt% Pt/XC-72R electrode, the hydrogen adsorption/desorption peaks from 1.5 wt% Pt/Y zeolite were different with no second adsorption peak observed. This difference indicated that the Pt nanoparticle size on Y zeolite was smaller than those on carbon-supported catalyst substrates. Conclusively, the characteristics of electrochemical reaction of a 15ancr4 electrocatalyst are consistent to that observed from a 5 wt% Pt/XC-72R catalyst.

3.4. In-situ EXAFS Experiment

Table 2 gives the results fitting for 1.5 wt% Pt/Y zeolite (15ancr4) electrocatalyst. The data was collected at a potential of -0.65 V in the hydride region at a room temperature, using electrochemical cell. The curve fitting for in-situ EXAFS measurement was only extended up to 3 shells with shell 1 and shell 2 fitted for Pt and shell 3 for oxygen. The Pt coordination numbers in the first and the second shells were approximately 7.45 and 2.05. Some improvements in data results fitting can be achieved by adding the third Pt-O shell. The Pt-Pt distance in the first shell was found to be 2.77 Å, indicating that Pt nanoparticles were metallic in nature and thus preserved the bulk Pt characteristics.

Table 2. The data fitting results for 15ancr4 electrocatalyst.

15ancr4	Shell 1 Pt	Shell 2 Pt	Shell 3 O
N	7.45	2.05	0.75
R/ Å	2.77	3.85	2.19

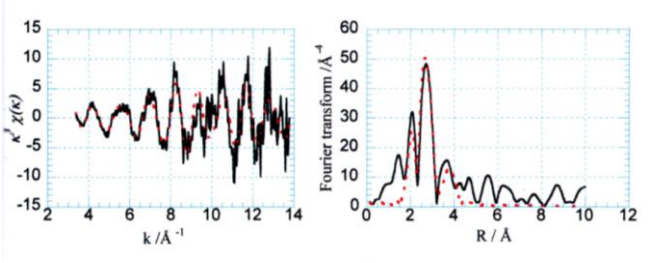

(a) Raw data (b) Fourier transformation

Fig. 5. EXAFS data fitting for 1.5 wt% Pt/Y zeolite catalysts with phase corrected with experimental data in black solid line and the fitted data in red dashed line. Data collected at a potential of -0.65 V vs MMS reference electrode under potential deposition.

Figure 5 illustrates the data fitting over the raw EXAFS (Chi) data ($k^3\chi(k)$ vs k/Å) and its Fourier transforms. It can be seen that the curve fitting (in dashed lines) matches the general form of the raw data (in solid lines) quite well. The Pt nanoparticle size determined in the hydride region of a potential -0.65 V is relatively small, compared to that obtained from the ex-situ EXAFS results fitting in air or hydrogen gas treatment cells. The oxygen coordination number observed for 1.5 wt% Pt/Y zeolite (15ancr4) electrocatalyst at -0.65 V upon the electrochemical reduction may be attributed to the fact that the Pt is in a direct contact with zeolite structure. It may also be related to the Pt oxide in a smaller cage, such as sodalite cage and hexagonal prism. Previous BET surface area measurements and XRD pattern characterization have confirmed that the loss of zeolite pore structure for Pt/Y catalyst occurs during thermal treatment. This might lead to Pt ions or atoms encaged in small cages where hydrogen molecules are found difficult to reach during chemical reduction process. The Pt catalytic active surface area on zeolite can be determined via hydrogen adsorption peaks represented in hydride region of CV. The calculation has resulted in 51.29 m^2/g Pt catalytic active surface area in the hydride region. However, the actual Pt active surface area on zeolite should be higher, as some of entrapped Pt atoms were unaccounted. Both CV measurement and in-situ EXAFS analysis provide some evidences of the presence of absorbed hydrogen species on Y zeolite during electrochemical reduction. The mobility of hydrogen and protons on zeolite structure can be explained using a hydrogen 'spillover' mechanism. H^+ and H_3O^+ are two most important species in hydrogen 'spillover' process [6, 18]. It is known that zeolite is a dc electronic insulator. H^+ 'spillover' can be transmitted along the surface of zeolite substrate to increase the surface conductivity of electrode. The zeolite acts as an electron bank to donate or receive electrons during the electrocatalytic reactions due to the presence of the acidic sites, such as the Bronstead or Lewis acid sites. During the chemical reduction process, hydrogen atom is initially absorbed on the Pt catalytic sites. The excess adsorption of hydrogen atoms can spill over within the zeolite structure, leading to a flow of protons along the acidic sites and then transport hydrogen species to the other Pt nanoparticles on zeolite. In electrochemical reduction process, H^+ ions are firstly reduced to form the adsorbed hydrogen, H_{ads}, on zeolite, and then desorbed from Pt catalytic sites to form hydrogen (H_2) molecules. This phenomenon has been supported by the presence of hydrogen adsorption/desorption features as seen in CV measurements.

4. CONCLUSIONS

An experimental study has been carried out to investigate the electrocatalytic characteristics of a 1.5 wt% Pt/Y zeolite in 2.5 M H_2SO_4 electrolyte solution, using cyclic voltammetry (CV) and the extended X-ray adsorption spectroscopy (EXAFS). From EXAFS data fitting, the Pt-Pt distance in the first shell of Pt is found 2.75 Å ~ 2.77 Å, indicating the metallic characteristics of the bulk Pt. Theoretical estimation shows 92% Pt dispersion on zeolite with an average of 13 atoms at the edge of a Pt cluster for an icosahedron structure. The Pt nanoparticle size is measured at 0.7 nm in an electrochemical cell, and at 1 - 1.1 nm in a gas cell with 147 and 55 atoms in a Pt cluster, respectively. The in-situ EXAFS analysis and electrochemical CV measurements of the hydrogen adsorption and desorption peaks in hydride region have confirmed that H^+ ions 'spillover' phenomenon is likely contributed to the electrocatalytic reaction on Pt/Y zeolite. The presence of hydrogen species adsorption on Pt might be due to either direct electron transfer or the mobility of H_{ads}/H^+ species. The H^+ ions can be transmitted on zeolite to increase the surface conductivity and transport hydrogen species onto Pt nanoparticle catalytic sites. Present study has confirmed that Pt nanoparticles located on Y zeolite can be electrochemically accessible; despite that zeolite is a dc insulator. The Pt/Y zeolite as a new type of electrocatalyst has shown some promises for practical industrial fuel cell applications in terms of cost reduction and efficiency improvement.

References

1. R.E. Benfield, J. Chem. Soc. Faraday Trans., 88, 1107-1110 (**1992**)
2. M.-K. Min, J. Cho, K. Cho and H. Kim, Electrochimica Acta, 45, 4211–4217 (**2000**)
3. D.W. Breck, Zeolite Molecular Sieves: Structure, Chemistry and Use, Wiley – Interscience Publisher, (**1974**)
4. D.R. Rolison, Chemical Review, 90, 867 (**1990**)
5. C.A. Bessel and D.R. Rolison, Journal of Electroanalytical Chemistry, 439, 9 –105 (**1997**)
6. P. Ueda, T. Kusakari, K. Tomishige and K. Fujimoto, J. Catalysis, 194(1), 14-22 (**2000**)
7. J. Wen, B.L. Wu and C.S. Cha, Journal of Electroanalytical Chemistry, 476, 101–108 (**1999**)
8. A. Zhang, I. Nakamura and K. Fujimoto, Journal of Catalysis, 168(2), 328-333 (**1997**)
9. B.I. Boyanov and T.I. Morriso, Journal of Physical Chemistry, 100, 16310-16317 (**1996**)
10. T. Yakoyama, N., Kosugi K. Asakura, Y. Iwasawa and H. Kuroda, Journal De Physique Colloques, 47, C8-273 (**1986**)
11. D.C. Koningsberger, J. de Graaf, B.L. Mojet, D.E. Ramaker and J.T. Miller, Applied Catalysis A: General, 191, 205-220 (**2000**)
12. L. Persaud, A.J. Bard, A. Campion, M.A. Fox, T.E. Mallouk, S. E. Webber and J. M. White, Inorg. Chem., 26, 3825-3827 (**1987**)
13. P. Gallezot, A. Alarcon-Diaz, J.-A. Dalmon, A.J. Renouprez and B. Imeuk, Journal of Catalysis, 39, 334-349 (**1975**)
14. G. Bergeret, P. Gallezot and B. Imelik, J Phys. Chem., 85(4), 411-416 (**1981**)
15. W.M.H. Sachtler and Z.C. Zhang, Advances in Catalysis, 39, 129-220 (**1993**)
16. J. Yao, PhD Thesis, Dept. of Chemistry, University of Southampton (**2001**)
17. C. Brett and M.A.O. Brett, Electroanalysis, Oxford University Press, (**1998**)
18. W.C. Conner and J. G.M. Pajonk, Advances in Catalysis, Academic Press, 34, 1 (**1986**)